R. Navid, J. R. Clark, M. Demirci, and C. T.-C. Nguyen, “Third-order intermodulation distortion in capacitively-driven CC-beam micromechanical resonators,” *Technical Digest*, Int. IEEE Micro Electro Mechanical Systems Conference, Interlaken, Switzerland, Jan. 21-25, 2001, pp. 228-231.

THIRD-ORDER INTERMODULATION DISTORTION IN CAPACITIVELY-DRIVEN CC-BEAM MICROMECHANICAL RESONATORS

Reza Navid, John R. Clark, Mustafa Demirci, and Clark T.-C. Nguyen
Center for Integrated Microsystems
Department of Electrical Engineering and Computer Science
University of Michigan
Ann Arbor, Michigan 48109-2122

ABSTRACT

The mechanism behind third order intermodulation distortion (IM_3) in capacitively driven clamped-clamped beam micromechanical (“CC-beam μmechanical”) resonators is shown to arise mainly from nonlinear interactions between applied off-resonance electrical signals and the mechanical displacements they induce. Analytical formulations for the third-order input intercept point (IIP_3) are then presented, first with simplifications that allow a closed form expression, then with additional complexities to account for second-order effects, such as beam bending due to an applied dc-bias voltage. Using this analytical formulation, predicted voltage IIP_3’s of 1.8V and 6.5V for 9.2 MHz and 17.4 MHz μmechanical resonators, respectively, closely match measured values of 1.8V and 6.3V. Extensive data on the dependence of IIP_3 on dc-bias voltage, resonator Q, and resonator center frequency, are also included to lend further insight into the trade-offs involved when designing for a specific linearity requirement.

I. INTRODUCTION

Despite recent increases in the frequency range of micromechanical resonators [1][2], and demonstrations of complex mechanical filtering circuits using such devices [3], efforts to apply μmechanical resonator technology to RF communication circuits have so far been delayed by lingering questions concerning the linearity of these devices, which must satisfy strict specifications for present-day cellular and cordless phone applications. For example, the European GSM standard for mobile communications requires a minimum total IIP_3 of –18 dBm in the receive path to insure adequate suppression of alternate-channel interferers [4].

Pursuant to determining whether or not μmechanical signal processors possess sufficient linearity for such applications, this paper presents a complete analytical formulation for the IIP_3 of capacitively driven CC-beam μmechanical resonators (c.f., Fig. 1), then verifies the formulation via measurement, where voltage IIP_3’s of 1.8V and 6.3V are observed for 9.2MHz and 17.4MHz μmechanical resonators, respectively. After a brief review of IM_3 and IIP_3, the analytical formulation is first presented in an intuitive form in Section III, then in a more complete form in Section IV. Section V then compares theoretical prediction with measurement.

II. BACKGROUND: IM_3 AND IIP_3

Third-order intermodulation distortion (IM_3) for a frequency filter occurs when system nonlinearities allow out-of-band signal components (tones) spaced from an in-band frequency ω_o by $\Delta\omega$ and $2\Delta\omega$, respectively, to generate an in-band component S_{IM3} back at ω_o [5]. This phenomenon can be illustrated quantitatively by applying an input containing the desired signal (i.e., the fundamental) plus the two out-of-band (interfering) tones, given by

$$S_{in} = S_i[\underbrace{\cos\omega_o t}_{\text{Fundamental}} + \underbrace{\cos\omega_1 t}_{\text{Tone 1}} + \underbrace{\cos\omega_2 t}_{\text{Tone 2}}] , \tag{1}$$

to the general nonlinear transfer function

$$S_{out} = A_o + A_1 S_{in} + A_2 S_{in}^2 + A_3 S_{in}^3 + \dots , \tag{2}$$

where $A_o, \dots, A_n$ are constants if the system is memoryless. Inserting (1) into (2), then expanding, yields (among other components)

$$S_{out} = \dots + \underbrace{A_1 S_i \cos\omega_o t}_{\text{Fundamental}} + \underbrace{\frac{3}{4} A_3 S_i^3 \cos(2\omega_1 - \omega_2)t}_{3^{\text{rd}}\text{-Order Intermod } (IM_3)} + \dots , \tag{3}$$

where an IM_3 component is seen to be generated via third-order nonlinearity represented by A_3.

For the common case where the interferers are located at frequencies $\Delta\omega$ and $2\Delta\omega$ from the fundamental (as shown in Fig. 2(a)), the quantity $(2\omega_1 - \omega_2)$ will be equal to ω_o, and the IM_3 component will be at the same frequency as the fundamental, possibly masking it if either A_3 or the interfering tone magnitudes are too large. In effect, as also illustrated in Fig. 2(a), even though the interfering tones are outside the filter passband, they still generate an in-band response—a highly undesirable situation for a filtering device designed to reject out-of-band signals. To suppress this effect, the third-order nonlinear term in (2) must be constrained below a minimum acceptable value in practical communication systems. Among the more useful metrics to gauge the ability of a system to suppress IM_3 distortion is the third-order input intercept point IIP_3, defined as the input amplitude S_i at which the extrapolated IM_3 and fundamental output components are equal in magnitude. In general, a large IIP_3 is preferred for communication applications.

III. FIRST-ORDER FORMULATION FOR IIP_3

Pursuant to determining the IIP_3 for the devices of this work, Fig. 1 presents the perspective-view schematic for a capacitively-driven CC-beam μmechanical resonator embedded in the measurement set-up to be used for verification in Section V. As shown, this

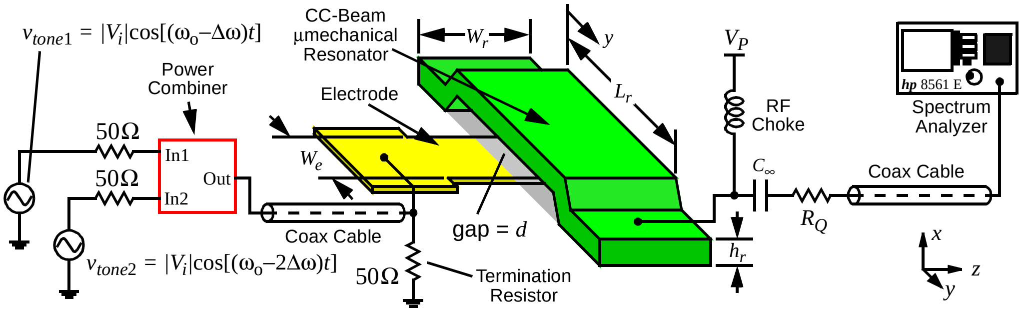

Fig. 1: Perspective-view schematic of a CC-beam μmechanical resonator in an IIP_3 measurement set-up.

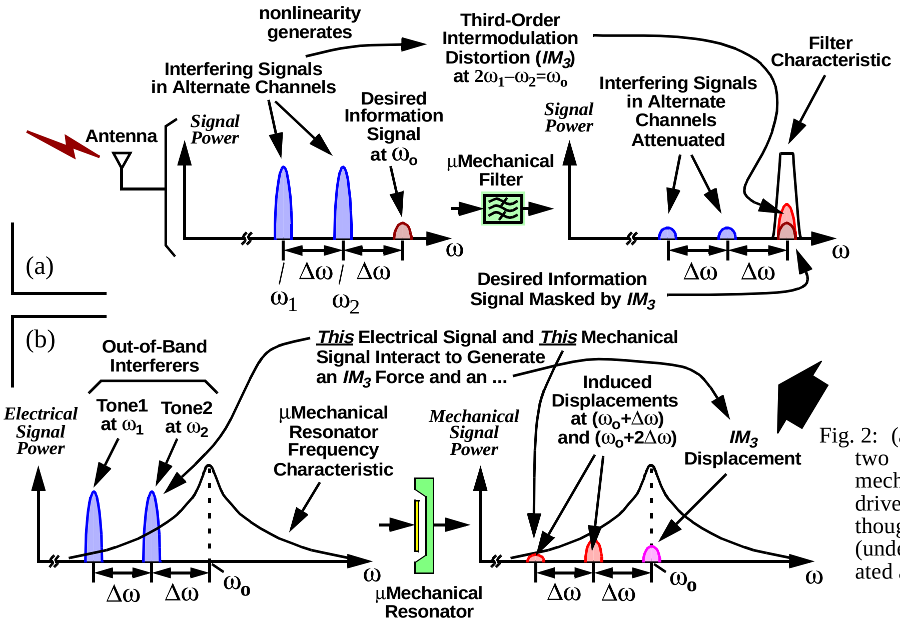

Fig. 2: (a) Schematic description of IM_3 generation by two interferers. (b) Schematic description of the mechanism for IM_3 generation in a capacitively-driven μmechanical resonator. Note here that even though there are no signals applied at resonance, an (undesirable) IM_3 output displacement is still generated at the resonance frequency.

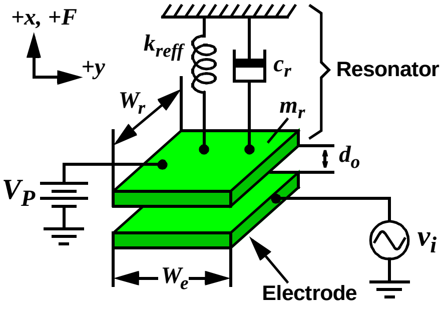

Fig. 3: Simplified lumped-parameter model for a capacitively-driven CC-beam for a first-order IIP_3 analysis.

device consists of a single conductive beam, fixed to the substrate at both ends, with a conductive electrode underlying the central portion of the beam. The electrode and beam essentially comprise the two plates of the transducer capacitor $C(x)$, across which an input voltage consisting of the sum of a dc-bias V_P and ac signal v_i are applied to drive the beam into vibration.

Because high frequency CC-beam μmechanical resonators generally vibrate with amplitudes much smaller than their lengths (e.g., 100Å amplitude for a 40μm-long beam), it is often not mechanical nonlinearity that governs the degree of IM_3 distortion seen, but rather nonlinearity in its capacitive transducer. In particular, $C(x)$ is quite nonlinear for VHF resonators due to the need for small electrode-to-resonator gaps [1]. Thus, as shown in Fig. 2(b), the mechanism for IM_3 distortion then involves nonlinear interplay across $C(x)$ between applied electrical interferer tones and the tiny off-resonance displacements they generate, giving rise to an in-band IM_3 force component (at $2\omega_1-\omega_2=\omega_o$).

A first-order expression for this IM_3 force component can be obtained by approximating the beam and electrode by the lumped mass-spring-damper equivalent shown in Fig. 3, where static bending of the beam caused by the applied dc-bias V_P has been neglected, and where expressions for the lumped elements can be found in [3]. For this simplified system, the total force acting on the suspended mass under an applied input V_P–v_i is given by

$$\begin{aligned} F_{tot} &= \frac{1}{2}(V_P-v_i)^2\frac{\partial C}{\partial x} = \frac{1}{2}(V_P-v_i)^2\frac{\partial}{\partial x}\left[C_o\left(1+\frac{x}{d_o}\right)^{-1}\right] \\ &= \frac{1}{2}(V_P-v_i)^2\left[-\frac{C_o}{d_o}\right]\left\{1-\frac{2}{d_o}x+\frac{3}{d_o^2}x^2-\frac{4}{d_o^3}x^3+\ldots\right\} \end{aligned} \tag{4}$$

where d_o and C_o are the electrode-to-resonator gap spacing and capacitance, respectively, when the beam is stationary, and where the final form comprises a Taylor expanded approximation. In (4), if v_i is composed of the sum of two off-resonance tone signals

$$v_i = V_1\cos\omega_1 t + V_2\cos\omega_2 t\,, \tag{5}$$

then the resulting displacement can be written as

$$x = X_1\cos(\omega_1 t+\phi_1) + X_2\cos(\omega_2 t+\phi_2) \tag{6}$$

where the values of X_1, X_2, ϕ_1, and ϕ_2, can be obtained from the voltage-to-displacement transfer function of the μmechanical beam

$$\frac{X(j\omega)}{V(j\omega)} = \frac{V_P}{k_{reff}}\frac{C_o}{d_o}\Theta(\omega)\,, \tag{7}$$

where

$$\Theta(\omega) = \frac{1}{1-(\omega/\omega_o)^2+j\omega/(Q\omega_o)}\,, \tag{8}$$

and where k_{reff} is the effective integrated stiffness at the midpoint of the beam [3].

Applying (5) and (6) to (4) with V_1=V_2=V_i, then expanding and collecting only IM_3 terms with frequency ($2\omega_1-\omega_2$), the expression for the IM_3 force is found to be

$$\begin{aligned} F_{IM3} = V_i^3\cdot\Bigg\{&\frac{1}{4}\frac{(\varepsilon_o A_o)^2}{d_o^5}\frac{V_P}{k_{reff}}[2\Theta_1+\Theta_2^*] \\ &+\frac{3}{4}\frac{(\varepsilon_o A_o)^3}{d_o^8}\frac{V_P^3}{k_{reff}^2}\Theta_1[\Theta_1+2\Theta_2^*]+\frac{3}{2}\frac{(\varepsilon_o A_o)^4}{d_o^{11}}\frac{V_P^5}{k_{reff}^3}\Theta_1^2\Theta_2^*\Bigg\} \end{aligned} \tag{9}$$

where ε_o is the permittivity in vacuum, A_o=W_rW_e is the electrode-to-resonator overlap area, Θ_1=$\Theta(\omega_1)$, and Θ_2=$\Theta(\omega_2)$.

By equating (9) with the fundamental force component

$$F_{fund} = V_P\frac{C_o}{d_o}V_i = V_P\frac{\varepsilon_o A_o}{d_o^2}V_i\,, \tag{10}$$

then solving the expression for V_i, the input voltage magnitude at the IIP_3 is found to be

$$\begin{aligned} V_{IIP3} = \Bigg\{&\frac{1}{4}\frac{\varepsilon_o A_o}{d_o^3}\frac{1}{k_{reff}}[2\Theta_1+\Theta_2^*] + \frac{3}{4}\frac{(\varepsilon_o A_o)^2}{d_o^6}\frac{V_P^2}{k_{reff}^2}\Theta_1[\Theta_1+2\Theta_2^*] \\ &+\frac{3}{2}\frac{(\varepsilon_o A_o)^3}{d_o^9}\frac{V_P^4}{k_{reff}^3}\Theta_1^2\Theta_2^*\Bigg\}^{-1/2} \end{aligned} \tag{11}$$

Equations (9) and (11) clearly show that for a given set of tone frequencies, ω_1 and ω_2, the IIP_3 can be increased by reducing V_P and A_o, and by increasing d_o and k_{reff}—all modifications that will increase the series motional resistance R_x of a μmechanical resonator. Thus, a clear trade-off between linearity and series motional resistance (which for matching purposes often must be small) exists for capacitively transduced μmechanical beam resonators.

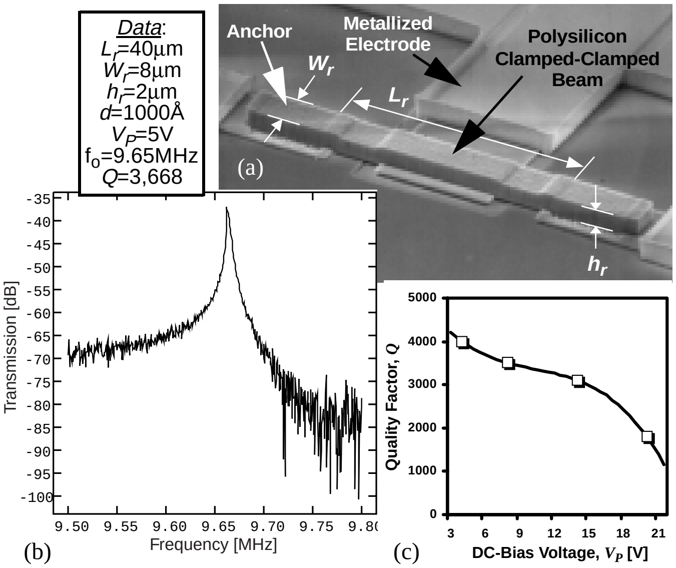

(b) (c)

Fig. 4: (a) SEM and (b) measured frequency response and numerical data for a 9.65 MHz polysilicon CC-beam µmechanical resonator. (c) Measured plot of Q versus V_P for this resonator.

IV. COMPLETE FORMULATION FOR IIP_3

Equation (11) clearly shows that the IIP_3 for a CC-beam µmechanical resonator depends heavily on the electrode-to-resonator gap spacing d_o. Thus, although (11) provides design insight and comes fairly close to the correct value for V_{IIP3}, it is not exact, since its derivation neglects the effect of beam bending due to the applied dc-bias V_P, which makes the gap spacing a function of location y. In addition, the use of a lumped rather than distributed k_{reff} also contributes an error.

To fully model these effects, expressions for $d(y)$ and $k_r(y)$ [3] must be used in the above derivation to attain F_{IM3} and F_{fund} as functions of y, which then must be integrated along the electrode width to obtain values for the total displacements X_{IM3} and X_{fund}. The V_{IIP3} is then found by equating these two total displacements and solving for V_i=V_{IIP3}. Although this procedure cannot be reduced to a single closed-form expression and so yields less design insight than (11), it does yield a more accurate value for V_{IIP3}.

V. EXPERIMENTAL RESULTS

CC-beam µmechanical resonators were fabricated using a polysilicon surface micromachining process similar to previous renditions [3], except for specific provisions to dope the electrodes n-type, but the resonator beams p-type. The use of different dopants for electrodes and structures was found to alleviate phenomena, such as depletion, that might otherwise increase the achievable gap spacing d_o over the target spacing [3]. Using this p/n-doping strategy, the CC-beam resonators of this work were able to match the target gap spacing of 1000Å much more closely than previous devices [3]. Figure 4 presents the scanning electron micrograph (SEM) of a 9.65 MHz CC-beam µmechanical resonator, along with a frequency characteristic and a curve-fitted plot of Q versus dc-bias V_P, both measured on a network analyzer under 50 µTorr vacuum achieved via a custom-built vacuum chamber.

IIP_3 measurements were made using the test set-up of Fig. 1, with $\Delta\omega=2\pi(200\text{kHz})$. As shown, interferer tones at f_o–200kHz and f_o–400kHz are combined, then applied to the input electrode of a CC-beam resonator to generate an IM_3 output response, which is measured at f_o via a spectrum analyzer. Figure 5 plots the fundamental and IM_3 output components versus the input voltage amplitude for a 9.39 MHz CC-beam µmechanical resonator biased as specified in the figure. From the intersection point in Fig. 5, the V_{IIP3} is seen to be 67.8 dBmV (or 2.45V).

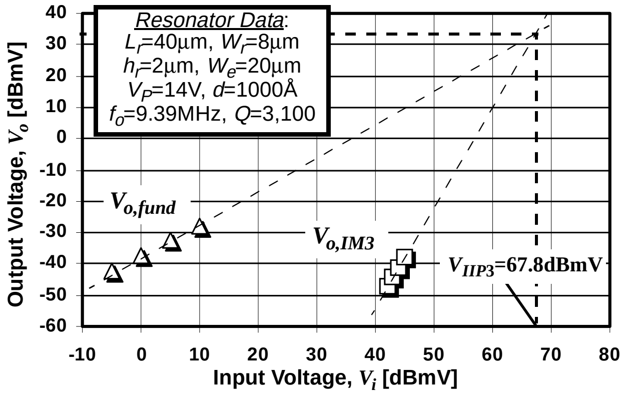

Fig. 5: Measured plot of V_o versus V_i for the µmechanical resonator of Fig. 4, showing an extrapolated V_{IIP3}=2.45V.

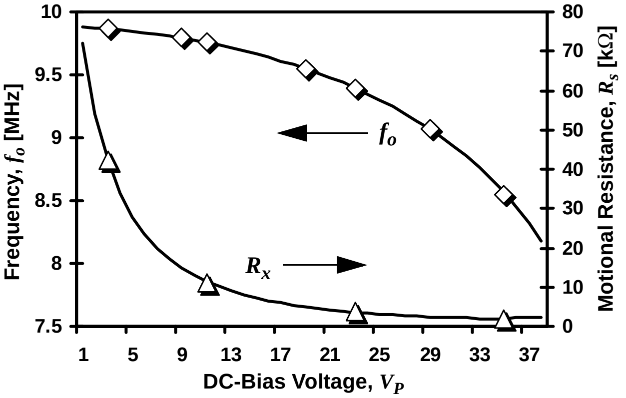

Fig. 6: Measured points and predicted plots of resonance frequency and R_x vs. V_p for a ~10 MHz CC-beam µresonator.

Given the very strong dependence of IIP_3 on the initial electrode-to-resonator gap spacing d_o (seen in (11)), it is important that d_o be known accurately to insure a sufficiently accurate theoretical prediction for comparison with measurement. To obtain an accurate value for the initial gap d_o, a plot of frequency f_o versus dc-bias V_P is measured, from which the value of d_o and the effective h are extracted via curve-fitting with a proven expression for f_o vs. V_P [3]. Figure 6 presents such a plot of f_o vs. V_P for a ~10 MHz CC-beam, obtained by measuring frequency characteristics such as in Fig. 4(a) for various values of V_P. By curve-fitting the measured points to a theoretical curve (shown in the figure) generated by Eq. (12) from [3], d_o is found to be 1029Å, and the effective h is 1.9µm. Using these values of d_o and h in Eq. (18) from [3], a curve for the series motional resistance R_x of this resonator is also plotted in Fig. 6, and this matches well with data taken from the measured frequency characteristics, giving further confidence in both the extracted value for d_o and in the models from [3].

To verify the accuracy of the formulation in Section IV, Fig. 7 plots measured and predicted values of V_{IIP3} versus V_P for a ~10 MHz CC-beam µmechanical resonator, showing very close agreement between measurement and theory. Note that Figs. 6 and 7 together verify the theoretical prediction of Section III that IIP_3 can be increased often only at the expense of increasing R_x.

Although V_{IIP3} is widely used for expressing IIP_3, some applications may prefer that IIP_3 be expressed as a power instead. The IIP_3 power P_{IIP3} can be determined from V_{IIP3} via the expression

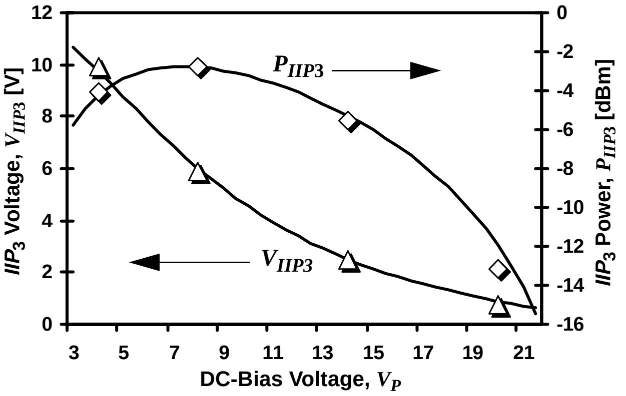

Fig. 7: Voltage and power IIP_3's vs. V_p for a ~10 MHz CC-beam µmechanical resonator.

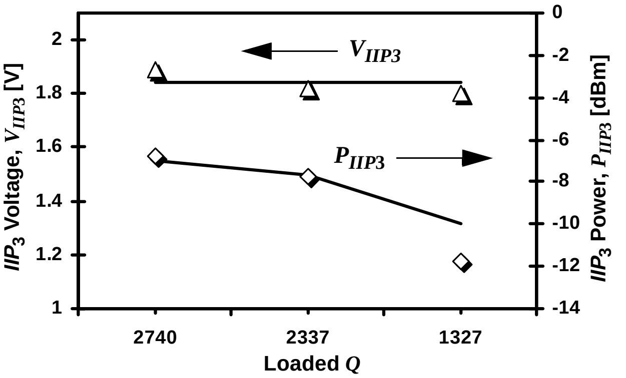

Fig. 8: Voltage and power IIP_3's versus Q for a ~10 MHz CC-beam µmechanical resonator.

$$P_{IIP3} = 10Log\left(\frac{V_{IIP3}^2}{2R_Q}\right) \tag{12}$$

where R_Q might, for example, represent a termination resistor needed in µmechanical filters to control the Q of filter end resonators [3]. Figure 7 also compares measured and calculated values (using R_Q=3R_x) for P_{IIP3}, showing that in contrast to V_{IIP3}, which decreases monotonically with increasing V_P, there is an optimum V_P at which the P_{IIP3} is maximized (at a value of –3 dBm). This can be explained by recognizing that as V_P increases, R_x decreases, hence R_Q decreases, leading to an increase in P_{IIP3}, as governed by (12). However, as V_P becomes even larger, the IM_3 force governed by (9) also steadily increases, due to both the direct increase in V_P and due to a decrease in d_o caused by V_P-induced beam bending. This latter effect begins to dominate after some threshold voltage V_P, beyond which the P_{IIP3} decreases with increasing V_P.

To quantify the dependence of IIP_3 on the loaded Q of a given CC-beam resonator, Fig. 8 presents a plot of both V_{IIP3} and P_{IIP3} versus Q for a ~10 MHz µmechanical resonator. To obtain this plot, the Q of the resonator was controlled by adding an R_Q resistor in series with the resonator. As seen from Fig. 8, V_{IIP3} remains relatively constant with Q changes, as predicted by (11) for interferers sufficiently far from the resonator center frequency; i.e., for $\Delta f >> f_o/(2Q)$. On the other hand, P_{IIP3} degrades with decreasing Q, even for distant interferers, as governed by (12).

Having verified (11) by comparison with actual measurements at frequencies near 10 MHz, projections for the IIP_3 values expected for even higher frequencies are now in order. In particular, given the direct dependence of V_{IIP3} on resonator stiffness k_{reff} shown in (11), the V_{IIP3} for a CC-beam is expected to increase as its resonance frequency increases. For example, the theory of Section IV predicts V_{IIP3}=19.6V for a 70 MHz CC-beam µmechanical resonator with Q=4000, V_P=27V, L_r=18.8µm, d_o=1000Å, h=3µm, W_e=L_r/2, W_r=10µm, and Δf=200kHz. On the other hand, although (11) and (12) also predict an increase in P_{IIP3} with resonance frequency, the expected increase is not quite as fast, since its rate of increase is counteracted by a simultaneous increase in R_x (hence R_Q) with frequency. For the example resonator above, with R_Q=3R_x, P_{IIP3}=+6 dBm—still adequate for most receive path applications in communications. Table I summarizes predicted and measured data for both the 10 MHz CC-beam discussed so far, and a 17.4 MHz CC-beam, clearly showing an increase in IIP_3 with frequency.

Table I: CC-Beam µMechanical Resonator IIP_3 Data

Parameter	9.2MHz	17.4MHz	Units
µResonator Dimensions: L_r, W_r, h	40,8,1.93	29,8,1.79	µm
Electrode Width, W_e	20	14	µm
Electrode-to-Resonator Gap, d_o	1,031	1,120	Å
DC-Bias Voltage, V_P	16	16	V
Quality Factor, Q	1,371	1,261	—
Measured Motional Resistance, R_x	8.46	23.77	kΩ
Predicted IIP_3 Voltage, V_{IIP3}	1.84	6.49	V
Measured IIP_3 Voltage, V_{IIP3}	1.8	6.27	V
Predicted IIP_3 Power, P_{IIP3}	–9.97	–5.27	dBm
Measured IIP_3 Power, P_{IIP3}	–11.77	–5.57	dBm

VI. CONCLUSIONS

Analytical expressions for the IIP_3 of capacitively driven CC-beam µmechanical resonators were presented and verified, showing IIP_3's as high as –3 dBm for a 10 MHz CC-beam terminated via an impedance 3X its own series motional resistance. (The P_{IIP3} is even larger for smaller termination impedances.) Although this measured value at 10 MHz easily satisfies GSM receive path requirements, it is still short of the +7.6 dBm needed for RF channel-selection in CDMA handsets (assuming a duplexer with >58 dB transmit power rejection precedes the µmechanical filter) [6]. Given that IIP_3 increases with frequency, according to the theory presented, this CDMA requirement should easily be achievable by a capacitively-driven UHF µmechanical filter. Whether or not µmechanical filters can eventually satisfy the duplexer requirement, on the other hand, is still the subject of ongoing research.

Acknowledgment: This work was supported under DARPA Cooperative Agmt. No. F30602-97-2-0101.

References:

[1] K. Wang, A.-C. Wong, and C. T.-C. Nguyen, "VHF free-free beam high-Q µmechanical resonators," *IEEE/ASME J. Microelectromech. Syst.*, vol. 9, no. 3, pp. 347-360, Sept. 2000.
[2] M. L. Roukes, "Nanoelectromechanical systems," *Tech. Digest*, 2000 Solid-State Sensor and Actuator Workshop, Hilton Head Island, South Carolina, June 4-8, 2000, pp. 367-376.
[3] F. D. Bannon III, J. R. Clark, and C. T.-C. Nguyen, "High frequency micromechanical filters," *IEEE J. Solid-State Circuits*, vol. 35, no. 4, pp. 512-526, April 2000.
[4] J. C. Rudell, J. A. Weldon, J. J. Ou, L. Lin, P. Gray, "An Integrated GSM/DECT Receiver: Design Specifications", UCB *Electronics Research Laboratory Memorandum,* Berkeley.
[5] B. Razavi, *RF Microelectronics*. New Jersey: Prentice Hall PTR, 1998.
[6] W. Y. Ali-Ahmad, "RF system issues related to CDMA receiver specifications," *RF Design*, pp. 22-32, Sept. 1999.